Indication of Ictal Propagation using Single Pulse Electrical Stimulation Evoked Early Responses

David Keizer

S0152110

Committee:

Prof. dr. M.J.A.M. van Putten

Dr. F.S.S. Leijten

Drs. P.A. van Katwijk

Prof. dr. S.A. van Gils

Dr. G.J.M. Huiskamp

Abstract

Early responses (<100ms) evoked by single pulse electrical stimulation (SPES) of the epileptic brain are thought of as physiological phenomena. This study investigates their relevance with respect to ictal propagation patterns. SPES and seizure data from eight patients were recorded with a sampling frequency of 512 Hz. Stimulation consisted of ten monophasic pulses on adjacent electrodes with a pulse width of 1 ms and a frequency of 0.2 Hz. Stimulus intensity varied between 8-4 mA depending on the occurrence of pain, twitches or after-discharges. A Wiener filter based algorithm removed stimulation artefacts and automatically detected responses. For each patient a recording of a single stereotypical, clinical seizure was obtained. Ictal propagation was marked by consensus of three experienced epileptologists. Sensitivity, specificity and predictive values for early responses were calculated with respect to the witnessed ictal propagation pattern. Our results show high mean specificity 0.91 (range 0.75-1.00) and a lower mean specificity 0.37 (range 0.21-0.65). However, in cases of low sensitivity we did find high positive predictive values for the early responses occurred, 0.68 (range 0.45-1.00). The mean negative predictive value was 0.73 (range 0.54-0.90). Our results suggest a relationship between early responses and ictal propagation patterns.

Preface

The road towards completion of this thesis has been long and winding. I want to take a moment here to thank everyone who has stood by me during this period. For either supporting me when needed or for giving me tough love whenever it was called for. Special thanks go out to my supervisors, my parents, Michel, Marjolijn and last but not least student councillor Hofman, whose advice kept my head on straight when it was most important. Again, thank you all for your patience and support, it has been invaluable.

Table of contents

General Introduction

Unravelling the inner workings of the human brain has long been a topic of scientific research. Especially finding out how different parts of the brain are effectively connected to each other has been widely investigated. It should be noted that a multitude of techniques have been developed over the years, originating from different fields of science. In this thesis we aim to gain new insights from early response data obtained from clinically indicated SPES recordings. The focus will be on effective connectivity in the epileptic brain and its relation to seizure propagation behaviour.

Chapter 1 – Comparing SPES and PLI

Introduction

Epilepsy is a common neurological disorder in which patients suffer recurrent epileptic seizures (i.e. events resulting from transient, hyper-synchronous, abnormal neuronal behaviour) [1]. These events can occur both provoked and unprovoked and can show a broad array of clinical manifestations depending on which part of the brain is affected and if the seizure is partial or general in nature. Symptoms range from altered perception of reality to large tonic-clonic seizures. Even though progress is made in developing new anti-epileptic drugs (AEDs), still ±20-30% of all patients are not fully controlled by drug therapy [2].

Imaging techniques can map the epileptic brain. Commonly applied modalities are MRI and fMRI. MRI can yield information on abnormal cortical morphology and fMRI can be used to visualize functional cortical areas like movement and speech [3-5].

Besides using imaging techniques to investigate the brain, electrophysiology driven methods are also investigated. For instance there is the method of applying an electrical stimulus to the brain and recording its response to this stimulus. We discriminate between the cortico-cortical evoked potentials (CCEP) and single pulse electro-cortical stimulation (SPES) [2, 6-10]. These similar techniques both apply a stimulus directly to the cortex, however they use a different stimulation paradigm.

Besides the above electrophysiological approach, math and statistics derived methods have also been developed [11-17]. These methods investigate interdependencies between different EEG and electro-corticography (ECoG) signals in terms of signal coherence, synchronization and phase locking to define connections between them. Resulting connections are often analysed through network theory. This application of such theory finds its origin in the conception that in epilepsy, abnormal activity is propagated through abnormal connections that constitute an epileptic brain network. Though many of these studies show interesting results, it should be noted that the definitions of connections between individual nodes in the network are often very different. As was critically reviewed by Fingelkurts et al. many of these definitions of functional connectivity draw heavily upon complex methodologies and frameworks of other fields of science in which operational conditions are clearly defined. In neuroscience many parameters are not fully known and sophisticated assumptions need to be made which do not always make sense in mathematical context [18].

When considering the mathematical and electrophysiological approaches to connectivity we wondered how our SPES data would compare to one of the mathematical notions of connectivity. In order to do so we set up an explorative pilot, comparing SPES stimulus-response effective connectivity to the phase lag index (PLI) [12].

Methods

For the descriptive analysis and comparison of SPES and PLI defined connectivity we analysed the data of two patients. ECOG recordings with a sampling frequency of 512 Hz were used. For the analysis of SPES and its responses a recording containing SPES stimulation data was used. PLI calculations were performed using a fragment of 8 seconds of artefact free interictal ECoG.

SPES responses were determined using an early version of the algorithm described in appendix A.

PLI values were calculated based on the methodology proposed by Stam et al. [12]. This connectivity measure quantifies the phase coupling between two time series as: $PLI = |\langle sign[\Delta\Phi(t_k)]\rangle|$ where $\Delta\Phi(t_k)$ is the phase difference between two time series and t_k are discrete steps [19]. The PLI only uses non-zero phase lags for its calculation, reducing the effect of volume conductivity. For an in-depth description of the PLI we refer to that article. Since PLI values are calculated for each electrode, a threshold needs to be applied to find the significant functional connectivity. This threshold value is not clearly given in literature. We defined the threshold in a way that the number of significant PLI values equalled the number of SPES responses in the analysed data.

Next we compared the occurrence of SPES early responses to the distribution of significant PLI values by means of an adjacency matrix. Anatomical distribution of the found connectivity is also examined.

Results

For the two patients the adjacency matrices were calculated. The results of which are shown below. Relevant anatomical distribution is also given.

Adjacency matrices

Shown are two examples of adjacency matrices. These images were designed to show a quick overview of the similarities between the SPES and PLI methodologies. At a first glance there seemed to be a striking absence of similarity between the two methodologies. PLI yielded a more diffuse, seemingly random distribution of its connectivity along the entire matrix. SPES responses showed a tendency to cluster around the diagonal (left image). Those were electrodes neighbouring the site of stimulation since the ECoG recordings were obtained using n x 8 strip and grid electrodes. It should also be noted that the recorded responses did not exclusively occur on neighbouring electrodes. Responses could also be seen on remote electrodes, this can readily be seen in the right image of figure 1.

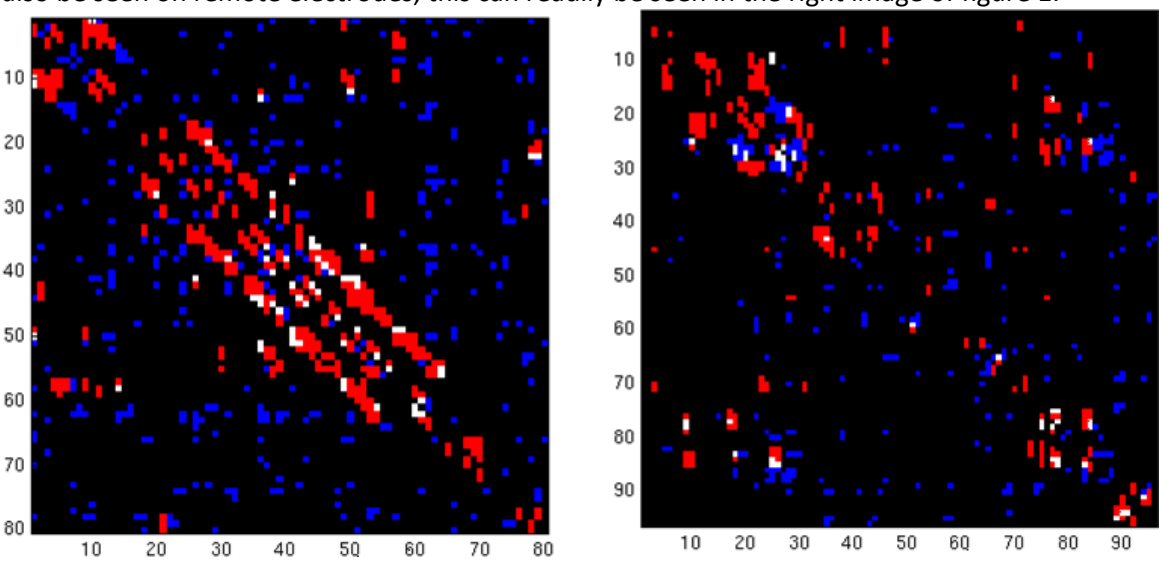

Figure 1 Adjacency matrices of two patients. Blue = PLI defined connectivity, Red = SPES stimulus-response relationship, White, occurrence of both PLI connectivity and SPES response. Channel numbers of stimulated electrodes are shown as rows, and channel numbers of electrodes showing a response can be read from the columns. PLI connectivity is by definition reciprocal, therefore there is no difference in rows/columns for the PLI.

PLI connectivity is by definition reciprocal. If electrode X has a consistent lag with respect to electrode Y, then electrode Y will have the same consistent lag with respect to X, save for a sign change. If we look closely at the SPES results, one could note that to some degree the matrix shows symmetrical properties.

Anatomical distribution

We also analysed the anatomical distribution of responses of the right image of figure 1 since the adjacency matrices do not give a feel for the relevance of these SPES responses.

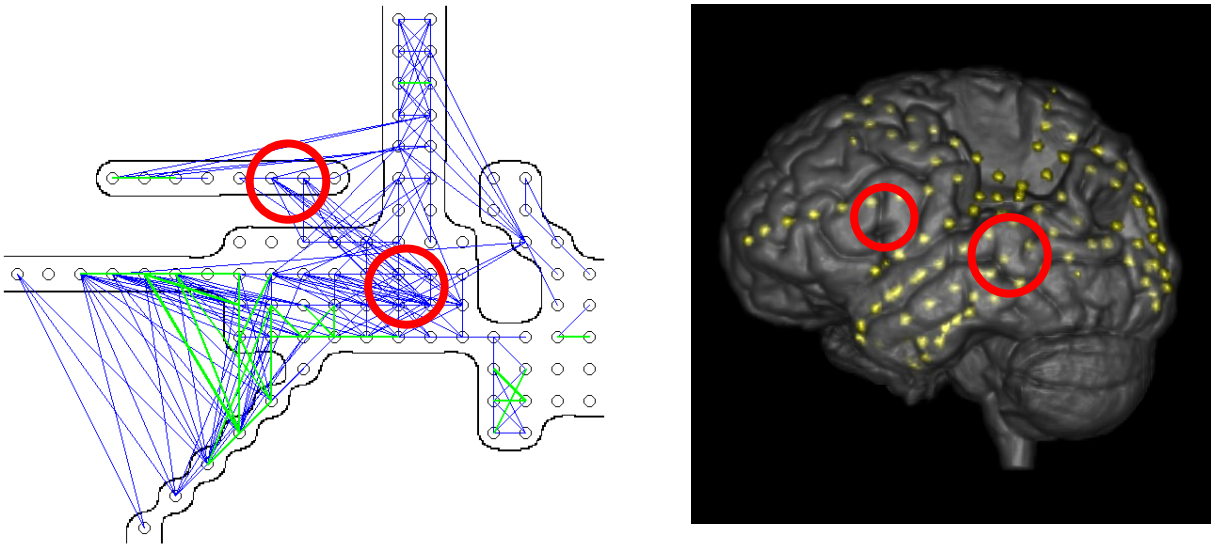

Figure 2 Anatomical distribution of the SPES early responses. Left a schematic representation, here stimulus response relationships are shown in blue lines. Green lines show the similarities between this patient's SPES and PLI results. Right shows the MRI image with the electrode positions in yellow. The red circles depict the stimulus response relationships between electrodes (left) that can be anatomically related to Broca and Wernicke's areas (right).

From figure 2 we can see that there is not a whole lot of similarity between the SPES and PLI results. What should be noted however is the fact that SPES has shown a stimulus-response relationship between areas most likely being Broca and Wernicke.

Discussion

From the results shown above it can be seen that major differences exist between both PLI and SPES data. From the small sample size in this preliminary study it was not possible to draw conclusions on the measure of similarity between them. However the results did raise interesting questions. For instance it is still unknown what processes are actually measured by PLI and what their relevance is in the context of epilepsy. Since PLI is derived from interictal ECoG and SPES is obtained from evoking responses from the brain we assumed that the 2 methodologies measure different underlying processes.

SPES early response results seem to have a very specific distribution. The occurrence of responses in the areas we know to be Broca and Wernicke's areas is also of note. Similar findings using evoked responses have been shown in CCEP literature [8]. If SPES is capable of mapping these known anatomical connections, what is the relevance of the other early responses evoked by SPES? In SPES literature a very clear distinction is made between early and delayed responses. Delayed responses are thought to be pathological in nature while the early responses are thought to be physiological in nature. Even if early responses are a purely physiologic phenomenon their distinct distribution patterns should not be ignored.

When epileptic seizures are considered we know that stereotypical seizures show very similar patterns of seizure propagation upon analysis of multiple ECoG recordings. From the results shown above we wonder if SPES evoked early response distribution might be related to the distinct propagation patterns seen in stereotypical seizures when the SPES is carried out in the seizure onset zone (SOZ).

Chapter 2 – SPES evoked early responses and seizure propagation

Introduction

Epilepsy is a common neurological disorder in which patients suffer recurrent epileptic seizures (i.e. events resulting from transient, hyper-synchronous, abnormal neuronal behaviour) [1]. These events can occur both provoked and unprovoked and can manifest itself in different ways depending on which part of the brain is affected and if the seizure is partial or general in nature. Symptoms range from altered perception of reality to large tonic-clonic seizures. Even though progress is made in developing new anti-epileptic drugs (AEDs), still ±20-30% of all patients are not fully controlled by drug therapy [2]. For this group of patients, surgical removal of the epileptogenic tissue can provide a possible curative solution [9, 20]. Accurate determination of what tissue should be removed is vital for good surgical outcome in terms of Engel classification and for sparing important functional areas of the brain [20]. To that extent a lot of work has been put into improving pre and peri-surgical analysis of the epileptic brain. MRI can yield information on abnormal cortical morphology, and fMRI can be used to visualize functional cortical areas like movement and speech [3-5]. However, these techniques lack the temporal resolution to accurately monitor epileptic activity (i.e. electrophysiological signal fluctuations over time cannot be properly registered). More recently an increase in electrocorticograpy (ECoG) monitoring is seen to further assist in delineating the epileptogenic cortex [2]. ECoG recordings use grids of subdurally implanted electrodes to measure electrical activity of the brain. Due to its high temporal and spatial resolution (i.e. a 1 cm inter-electrode spacing) it can yield information important for localizing the seizure onset zone. Besides considering the ECoG as an invasive version of the extracranial EEG (e.g. looking for interictal spikes and analyzing seizure onset) the implanted electrode grids offer the possibility of direct cortical stimulation [9]. Single-pulse electrical stimulation (SPES) evokes electrocortical activity in which early responses, delayed responses (>100 ms after the stimulus) and evoked high frequency oscillations (HFOs) can be identified [21]. Delayed responses and HFOs have already been shown to be potential markers for the epileptogenic cortex [9]. Furthermore, pre- and post-surgical analysis of the presence of HFO generating areas has shown a correlation between the removal of HFO generating areas and favourable surgical outcome [22].

Early responses to cortical stimulation had initially been proposed to be just physiological phenomena originating from the stimulation of cortico-cortical association fibres also known as u-fibres [23]. This was confirmed by a study combining fibre-tracking MRI and CCEP, relating response amplitudes to association fibre density in the language system [24]. This led to an increase in the use of cortical stimulation in the field of functional connectivity mapping [7, 8, 24, 25]. In cortico-cortical evoked potential (CCEP) studies, applying a slightly different stimulation paradigm than SPES, early responses have been used to map functional connectivity in the language and motor systems [7, 8, 24]. Furthermore early responses correlated to the connectivity found in resting state fMRI [6]. Opposed to the concept of being purely physiological in nature, early responses have been shown to have increased amplitudes when stimulated within the seizure onset zone [6]. Furthermore Enatsu et al. found that early response amplitudes are significantly higher in areas of ictal propagation [10]. However no efforts were made to use this knowledge to investigate the localizing value of early responses in defining the areas of ictal propagation.

With SPES we can stimulate the cortical neurons involved in the normal fibre projections as well as the neurons involved in pathological neuronal connections caused by the process of epileptogenesis.

Seizures have been shown to propagate through both neocortical pathways and association fibres [23, 26]. Furthermore, early response amplitude has been shown to be correlated to association fibre diameter [24]. Therefore we hypothesize a relationship between ictal propagation and localization of early responses elicited by stimulation of the seizure onset zone. If SPES early responses are a good indicator for ictal propagation they could help improve mapping of the epileptic brain during surgery, yielding information about epileptic seizures without them even occurring. We aim to investigate the feasibility of predicting ictal propagation through the use of SPES early responses.

Methods

Patients

Chronic electrocorticography data from eight patients suffering from intractable epilepsy admitted to the UMCU for surgical resection of the presumed epileptic focus were selected. Implantation of subdural electrodes was part of the pre-surgical evaluation of these patients. As part of this pre-surgical workup SPES was also applied and visually inspected. The selection of eight patients was made based on the availability of these SPES recordings. The inclusion criteria were: having an identical stimulation paradigm, absence of excessive 50 Hz noise, uniform recording equipment, having a sample frequency of 512 Hz and being recorded using a 22 bits high dynamic range. Further information on the patients' epilepsies are shown in table 1. From each patient two recordings were extracted from the database; one ictal recording containing a representative (stereotypical) seizure, and a recording of a full SPES stimulation session.

Table 1 Patient data

Patient	Sex	Age	Lateralisation	Onset
1	V	23	L	Subtemporal
2	V	17	R	Frontal
3	M	8	R	Parietal
4	V	18	L	Frontal
5	V	15	L	Parietal
6	M	26	L	Temporal
7	M	42	L	Temporal
8	V	27	L	Temporal

Electrocorticography

All patients were implanted with platinum silicon embedded electrode grids and strips (Ad-Tech). All electrodes had a contact surface of 4.2 mm^2 and an inter-electrode spacing of 1 cm. Electrode placement was performed based on clinical indication in a way that both the suspected epileptogenic regions and possible adjacent functional areas were covered. The number of implanted electrodes varied between the different subjects (range 80-120).

Single Pulse Data Acquisition

Pairs of neighbouring electrodes were stimulated. The stimulation protocol consisted of ten monophasic pulses with a pulse width of 1 ms and a frequency of 0.2 Hz. Initially the stimulus intensity was set to 8 mA. In case of pain, twitches or epileptiform after-discharges the intensity was reduced to as low as 4 mA.

Analysis of Clinical Recordings

Analysis of the ictal recordings was performed individually by three experienced epileptologists. They were asked to define a single electrode on which the first ictal activity occurs. Early ictal activity was defined as the first electrocorticography pattern consisting of rhythmic spikes, rhythmic sharp waves, spike and low wave complexes, increasing gamma activity, regular or sharpened delta or theta activities or low-amplitude activity in the beta range prior to the clinical manifestation of the seizure. Furthermore they were asked to mark all electrodes on which seizure propagation (i.e. ictal activity) was found within the first 30 seconds after initial onset. Whenever a seizure was found to progress into a generalized seizure they were asked to mark all electrodes showing ictal activity up to the point

where the seizure generalizes. Cases in which onset or propagation observations did not match were solved by a joint analysis in which consensus was reached.

Analysis of SPES data

For the analysis of SPES data we analysed the responses to stimulation of the seizure onset zone as defined by the epileptologists. Since the SOZ was defined as a single electrode and the stimulation was carried out bipolar a stimulation pair needs to be selected for analysis containing that single marked electrode. This selection was performed based on the anatomical position of the electrodes. When possible, a stimulation pair that was situated above a single gyrus was chosen. In cases where this could not be verified the choice was made to take the stimulation pair that showed the largest number of responses. This was done due to the notion that when one electrode in a stimulus pair is located above a sulcus the less efficient stimulation probably results in a smaller number of responses. We devised an algorithm capable of automatically detecting and quantifying SPES evoked early responses. Efforts were made to remove the stimulus artefact from the recordings since these artefacts can contaminate the early responses, causing amplitude offset (an example of a stimulation artefact is shown in figure 1). Re-referencing to an intracranial electrode was not an option since the stimulation artefact does not have an identical amplitude in all channels. Therefore doing so would induce new artefacts in the data. We first obtained the ten pulse averaged response on each individual electrode to reliably correct for the stimulation artefact. A template based artefact removal algorithm based on the Wiener filter was written since general morphology of the stimulation artefact was seen to be similar on all channels. This process assumes knowledge about the artefact that is to be removed, though the defined template for that does not necessarily have to be a perfect fit to the actual data. For this methodology it was imperative to define an artefact template that was as clean (i.e. not contaminated with occurring early responses) as possible. We first defined an initial estimate to acquire this clean artefact template. The initial estimate was defined as the average of all ten pulse averaged responses on all channels since we had a large number of electrode recordings (up to 128) and the number of electrodes not showing an early response was greater than the number of electrodes that do. This removed most of the stimulation artefact, making detection of the largest early responses feasible. To improve the quality of our template we performed a quick peak detection to find early responses. Subsequently a new template was defined. This time the ten pulse averaged responses of all channels not showing a response on the initial early response detection are used. This process was repeated four times to further refine the artefact template. After removal of the artefact, occurring early responses (within <0.1s after the stimulus) were detected by using a peak detection algorithm with an amplitude threshold defined by visual inspection of the artefact corrected data. The choice of amplitude threshold was made prioritizing sensitivity. When clear responses were not adequately detected due to an inadequate amplitude the threshold setting was lowered by 10uV steps. Threshold settings are reported in the results section. Further information on the applied algorithms can be found in appendix A.

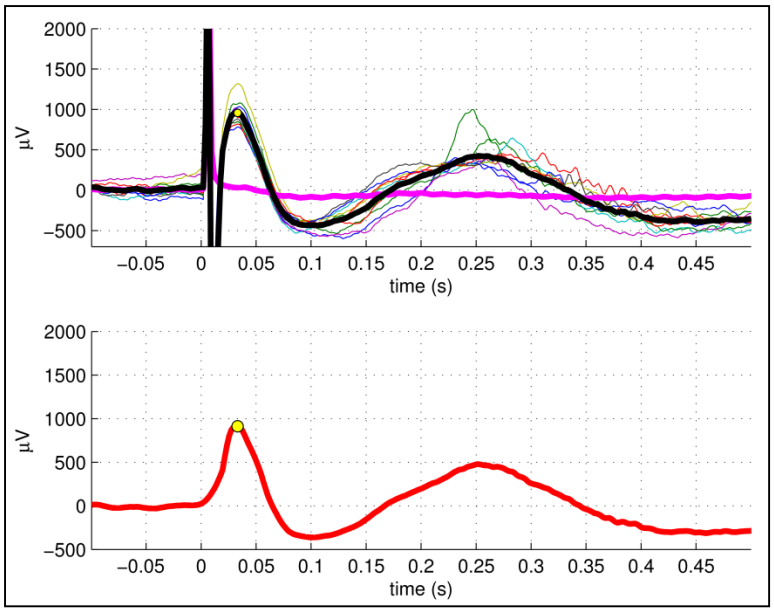

Figure 1 Example of a responses to stimulation, the averaged ten pulse response (black) the Wiener filter estimate of the stimulation artefact (purple) and the artefact free response (red).

From the pilot preceding this study we observed that SPES responses often occurred on electrodes adjacent to the site of stimulation. Responses on remote electrodes were often more localized and showed less activations adjacent to them. They did have similar morphology to the responses found in the vicinity of the stimulation site. We hypothesized that this could be attributed to the response amplitude being lower in amplitude than the actual stimulus. This lower amplitude may not be enough to evoke responses in the tissue surrounding a given response electrode. However, during the high amplitude electrical activity present during an epileptic seizure, local amplitudes might become large enough to evoke secondary local activity (i.e. a secondary hub effect).

We added an *adjacency correction* for SPES responses to deal with this phenomenon. This correction was implemented as follows. When a stimulation did not evoke a response in an electrode marked as being involved in the propagation of the actual seizure, a check was performed if an adjacent electrode that did show a response was involved in the defined seizure propagation. If this was the case it was thought the lack of a response on the first electrode could be due to the secondary local propagation phenomenon stated before. Non-responding electrodes adjacent to electrodes marked as true positive (see below) were taken along in the analysis.

Statistical analysis

In order to investigate how the spatial distribution of the single pulse evoked early responses compares to the actual seizure propagation we performed a sensitivity and specificity calculation. In this calculation we define each electrode as being:

- True positive - Seizure propagation and a detected early response
- False positive - No seizure propagation but a detected early response
- True negative - No seizure propagation and no early response detected
- False negative - Seizure propagation but no early response

From this the sensitivity and specificity are calculated as:

- $Sensitivity = \frac{n_{true\ positive}}{n_{true\ positive} + n_{false\ negative}}$

- $Specificity = \frac{n_{true\ negative}}{n_{true\ negative} + n_{false\ positive}}$

To investigate the actual predictive value of single pulse responses with respect to the ictal propagation we defined the positive (PPV) and negative (NPV) predictive values as follows:

- $PPV = \frac{n_{true\ positive}}{n_{true\ positive} + n_{false\ positive}}$

- $NPV = \frac{n_{true\ negative}}{n_{true\ negative} + n_{false\ negative}}$

Note that the suggested adjacency correction will not influence PPV and NPV results, since these are calculated using only the detected responses.

Results

In the eight patients data were recorded from an average of 98 electrodes (range 84-120). These numbers were corrected for silent electrodes caused by overlapping of grids, thus effectively causing insulation from the underlying cortex. Responses detected had a median response time of 43 ms (range 23-96ms) and a median response amplitude of 223 µV (range 106-1387 µV). Initial sensitivity calculations resulted in a mean sensitivity of 0.37 (range 0.21-0.65). Upon further inspection of the data the additional adjacency correction was applied as described in the methods section. This mean adjacency corrected sensitivity was 0.6 (range 0.33-0.88). Mean specificity was not affected by the added adjacency corrected sensitivity calculation, hence a single value calculated as being 0.91 (range 0.75-1.00). Mean PPV and NPV values were calculated as 0.68 (range 0.45-1.00) and 0.73 (range 0.54-0.90) respectively. An overview of the results for the individual patients can be found in table 2.

Table 2 Overview of the data characteristics of the analysed patients. Threshold values are shown in µV.

Patient	Number of electrodes	Response delay (ms)	Response Amplitude (uV)	Sensitivity	Adjacency Corrected Sensitivity	Specificity	PPV	NPV	Detection Threshold
1	93	64 (35-96)	378 (123-1387)	0.41	0.62	0.75	0.50	0.68	120
2	116	35 (23-88)	262 (106-428)	0.25	0.33	0.93	0.55	0.78	90
3	88	47 (23-92)	355 (132-1013)	0.24	0.48	0.98	0.91	0.60	140
4	79	44 (23-84)	443 (138-1193)	0.65	0.88	0.84	0.52	0.90	120
5	96	59 (35-82)	299 (152-698)	0.40	0.66	1.00	1.00	0.72	120
6	120	44 (23-96)	286 (147-694)	0.21	0.49	0.94	0.58	0.76	140
7	84	39 (23-49)	206 (120-333)	0.30	0.60	0.97	0.93	0.54	120
8	104	46 (23-82)	301 (136-876)	0.48	0.76	0.86	0.45	0.87	130

In the upcoming sections the results of the individual patients will be further discussed. For understanding of the visualized results figure 2 shows the global legend, which applies to all shown results.

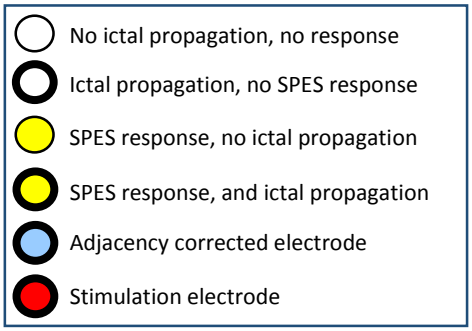

Figure 2 Global legend, applying to all subsequent topographical SPES response maps

Patient 1

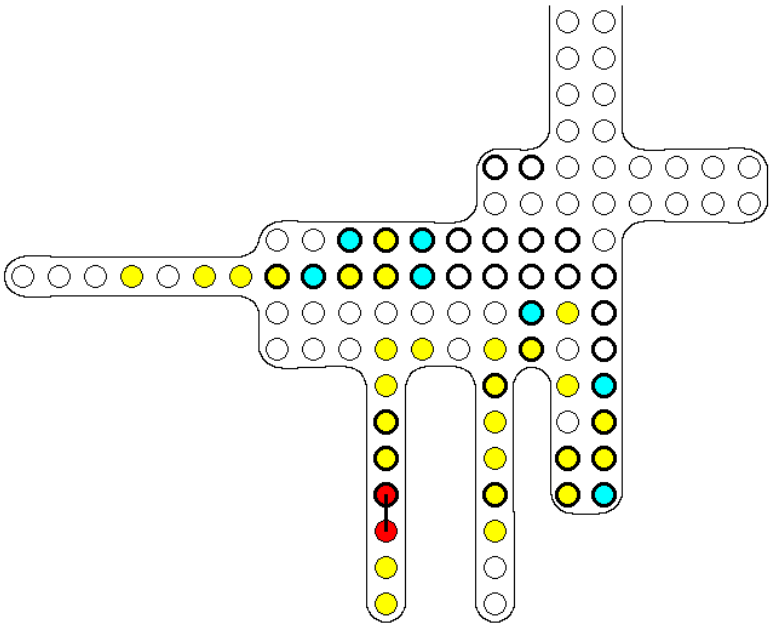

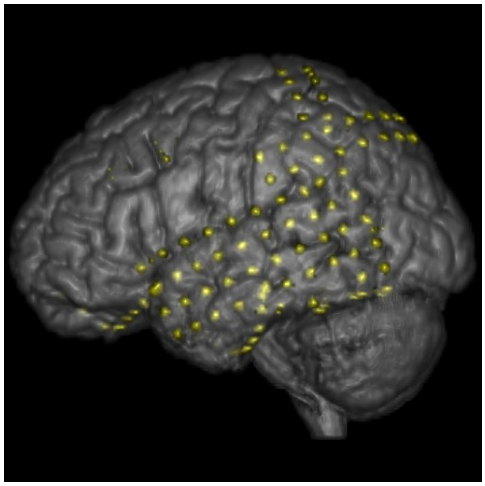

The first patient was found to have a seizure onset zone in the subtemporal area of the left temporal lobe. Mostly lateral and posterior temporal areas were marked as being involved in the propagation of the seizure. Notably the responses found were located in these same anatomical regions. On the superior part of the temporal grid numerous of electrodes marked as involved in the ictal propagation can be seen, but very little early responses were found. This could be explained by their position just above the sylvian fissure, rendering them unable to pick up the relatively low amplitudes of the early responses in that area but still capable of recording the high amplitude signals during the ictal phase.

Patient 2

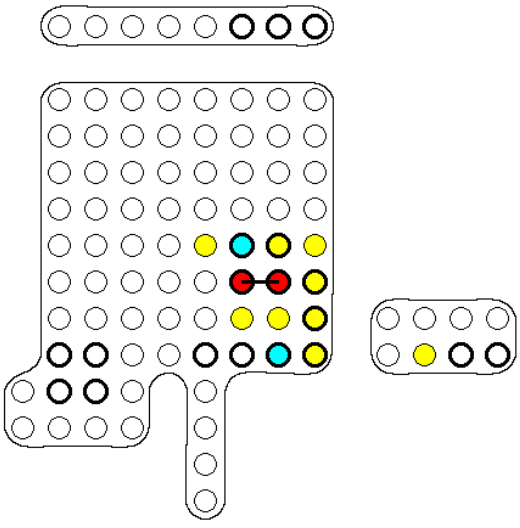

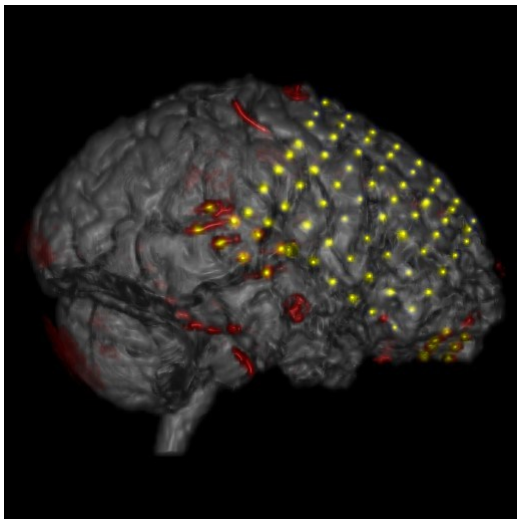

This patient had a fronto-lateral seizure onset zone with propagation to the posterior parietal, interhemispheric and fronto-orbital areas. The interhemispheric strip was situated right above the frontal grid but is not visible on this MRI rendering. Detected early responses have a local character, most of them located in the direct vicinity of the stimulation site. A single response was found in the fronto-orbital region, though just outside of the area involved in the seizure it does suggest that the

seizure onset zone has some connectivity with that region. Looking at the placement of the electrode grids it can be seen that around the seizure onset zone a lot of electrodes are located above a sulcus. This could result in sub-optimal stimulation causing a lack of more remote responses.

Patient 3

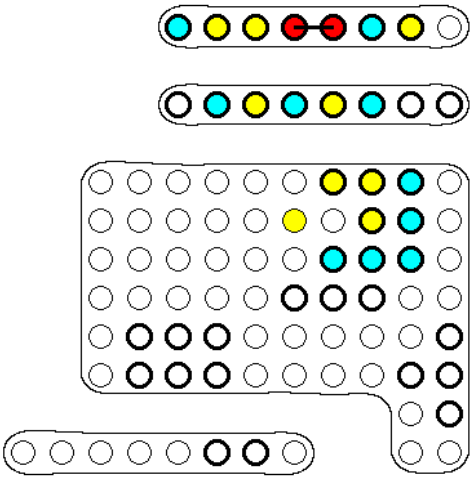

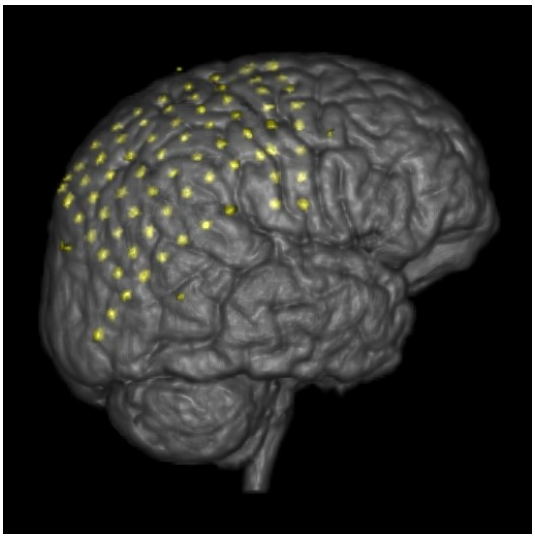

This patient had two interhemispheric strip electrodes implanted, the upper one directed more toward the frontal lobe and the bottom directed to the posterior regions. It should be noted that the seizure onset zone shown on the interhemispheric electrode was anatomically located close to the upper right electrodes of the parietal grid. There was some discussion on whether the onset was interhemispheric or parietal. While the consensus was reached on the interhemispheric onset the parietal involvement in the early stages of the seizure was evident. Early response localization was mainly in the interhemispheric areas though some responses were found in the parietal region. It was that exact same region that was involved in the early ictal phase.

Patient 4

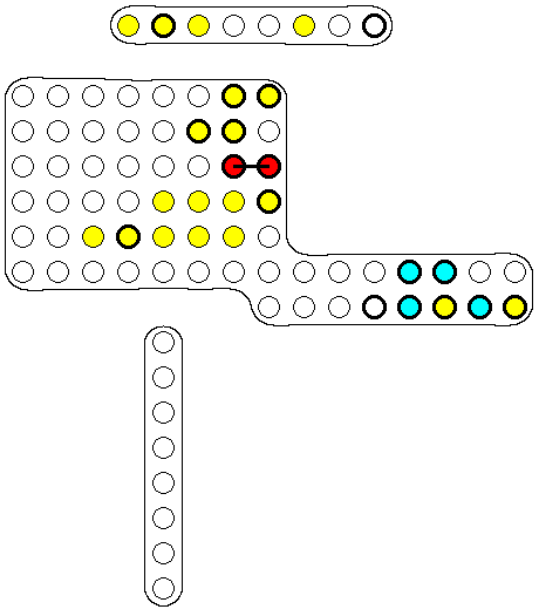

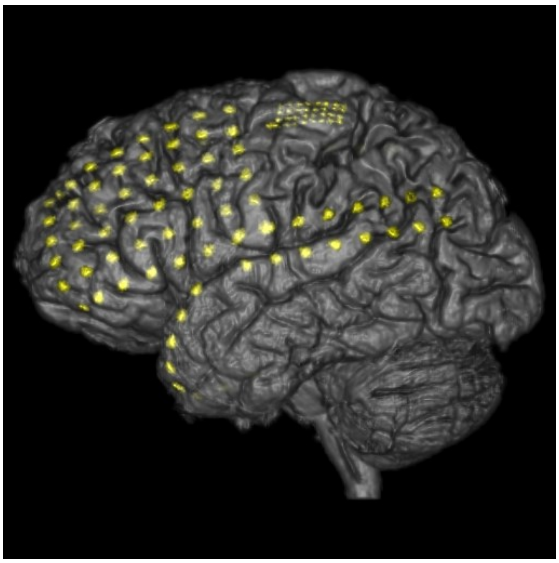

This patient with a frontal located onset zone showed propagation to the interhemispheric and parietal regions. Early responses can be seen to follow the same distribution with responses in both the immediate neighbourhood as well as responses in remote areas. Not every electrode marked as involved in ictal propagation showed a clear response but electrodes showing a clear response were found nearby.

Patient 5

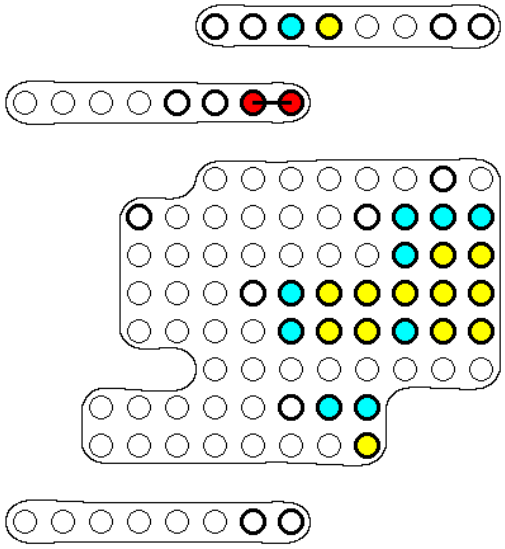

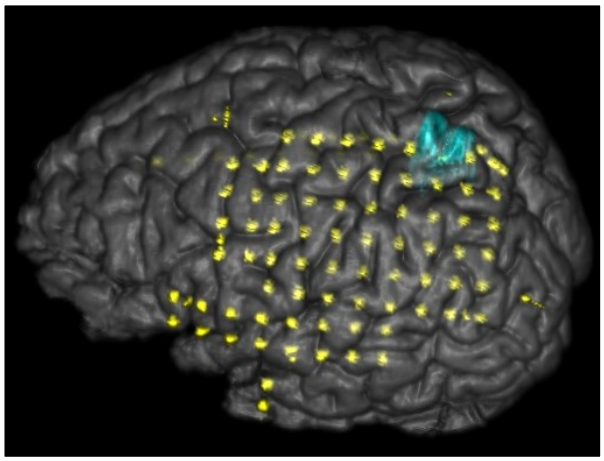

In this patient two interhemispheric strip electrodes were placed. One oriented more to the frontal regions and the other reaching more posterior regions. The onset was witnessed to occur on the frontally oriented interhemispheric strip. The responses however showed a marked spread to the remote areas of the parietal lobe. This is in concordance with the behaviour of the epileptic seizure. A single response located near the temporal lobe was also witnessed. Not every electrode marked as

involved in the seizure propagation showed a SPES response but the responses that do occur were found in the same general regions as the actual seizure propagation.

Patient 6

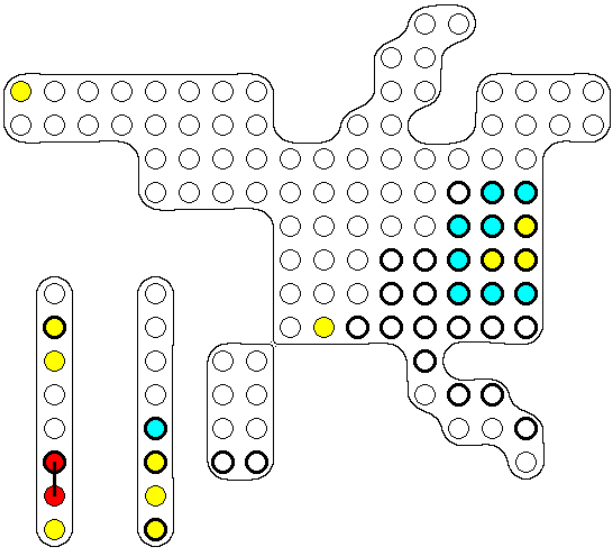

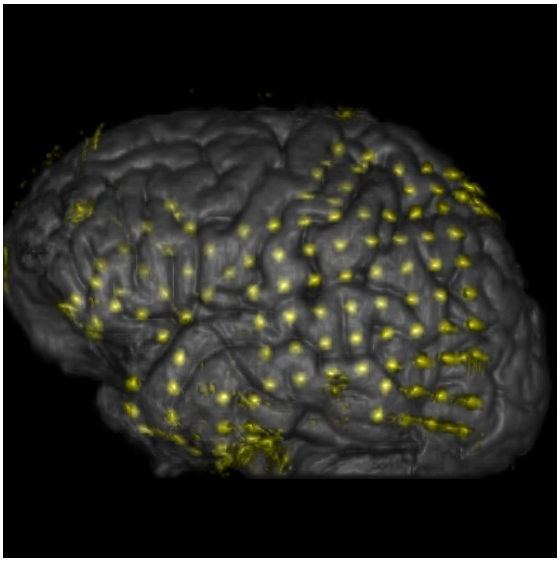

The subtemporal onset in this patient results in ictal activity over a relatively long distance with posterior temporal and parietal areas being affected. Even though single pulse responses are not seen in the majority of these affected electrodes, causing low sensitivity, the responses that are seen are of note. These occur in the core of the posterior temporal region that did show ictal activity. The effective connection between this region and the seizure onset zone suggests it could function as a site of secondary propagation.

Patient 7

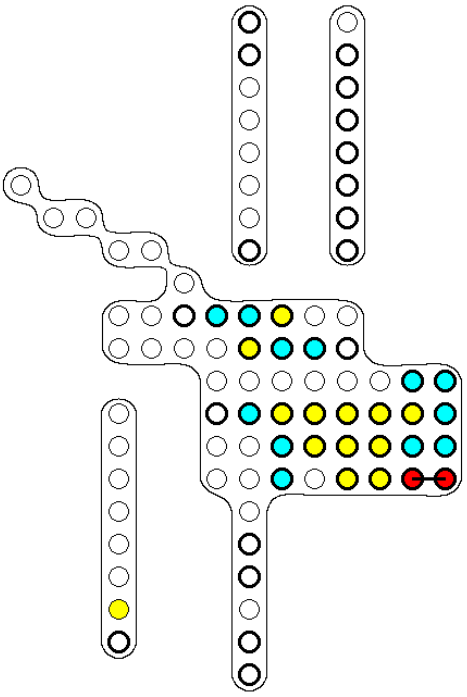

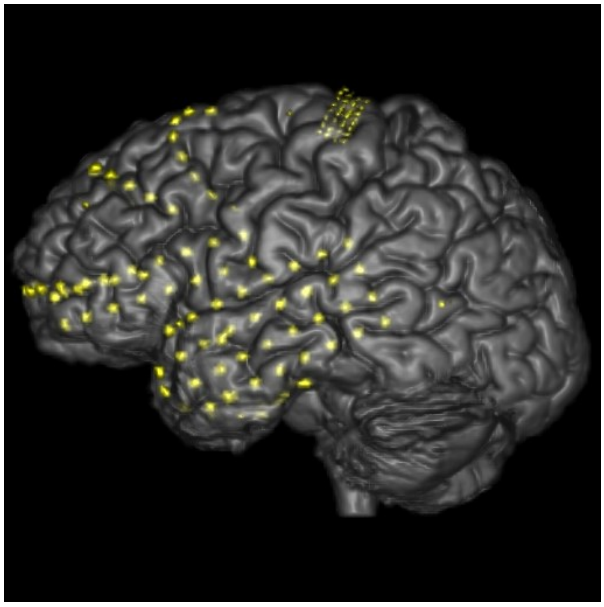

This temporal lobe epilepsy shows a propagation over the majority of the lateral temporal cortex with additional areas of activity being found in the frontal lobe. While single pulse evoked early responses are found mainly in the temporal lobe, the more remote higher frontal areas remain silent. On 2 frontal electrodes a response was found. Their localization could be attributed to some fibres of the arcuate fasciculus being stimulated and thus showing activations following known anatomical connections between the parietal and frontal lobe.

Patient 8

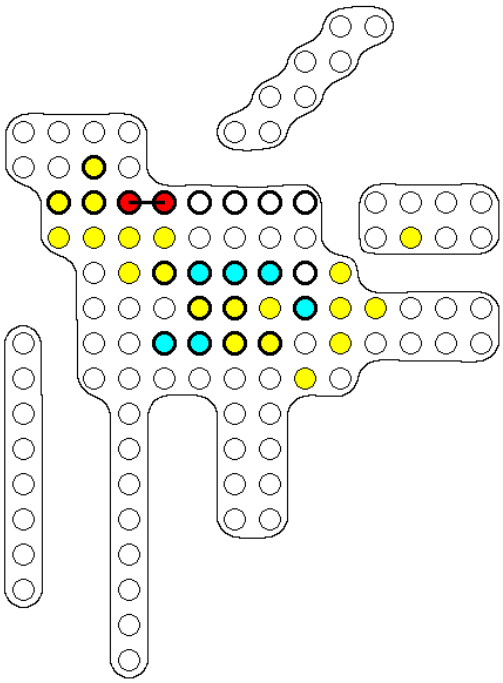

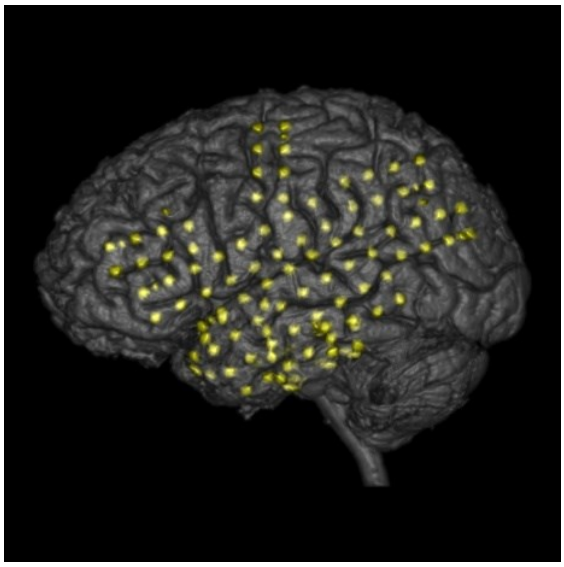

In this patient the seizure onset zone was determined to be around Broca's area. As one would suspect the responses were found in the temporal area corresponding to Wernike's area, with further responses along the temporal lobe. Local responses can also be seen in the frontal lobe around the site of stimulation. When compared to patient 7 it should be noted that Broca-Wernike connectivity is reciprocally shown, albeit in separate patients.

Discussion

We developed a method to compare the localization of the SPES early responses to the ictal propagation within the first 30 seconds of the seizure. This method showed that there is a clear relationship between these two phenomena, especially when we take into consideration that 30 seconds is a long time in terms of an epileptic seizure.

In the process of seizure propagation numerous electrophysiological modulating mechanisms are involved. The SPES protocol on the other hand uses the electrical pulses to map effective connectivity. The similarity between the localization of these two processes suggests that an epileptic seizure follows the strong anatomical and physiological pathways already present in the brain and that SPES can mimic its behaviour while circumventing some of the modulating processes active in the ictal phase.

Our results show a high specificity for response localization compared to seizure propagation. This means that it is rare to find single pulse responses outside of areas the seizure propagates towards.

Relation to findings in other research

SPES is related to CCEP studies since both investigate cortico-cortical responses to electrical stimulation, though both use a different stimulation paradigm. CCEP studies have also investigated the relationship between their so called N1 responses (i.e. the CCEP variant of the SPES evoked early responses) and epilepsy. In one of those studies they investigated CCEPs evoked in the SOZ (iCCEPs) to those evoked outside of the SOZ (nCCEPs). They found a statistically higher amplitude for N1 peaks in iCCEPs compared to nCCEPs [6]. This study found response amplitudes that were slightly higher than the ones we found in our results. This is explained by the fact that they only included the electrode showing the maximum N1 amplitude into their analysis. No further data ranges were given so there was little else to compare our results to. It should be of note however that in their nCCEP results they found numerous patients in which stimulation outside of the SOZ yielded no measurable evoked responses. In contrast, in our results we found ERs on nearly all stimulated electrode pairs upon visual inspection. A possible explanation for this lies in the fact that this study used a fairly limited cortical electrode coverage, therefore responses outside of the measured area could have been missed. A second explanation can be found in the difference in stimulation paradigm between SPES and CCEP. In the CCEP protocol a shorter pulse width is used (0.3ms compared to 1ms in SPES stimulation). Given a stimulation intensity similar to SPES (1-15mA) this results in a lower amount of injected charge into the cortical tissue. Furthermore in this same study they demonstrated a close relationship between stimulation intensity and response amplitude. Given the decrease in pulse width under similar stimulation intensity the reduction in total amount of injected charge might explain them missing possible responses due to low amplitude.

In another CCEP study they investigated the relationship between ictal propagation and CCEPs [10]. They compared the amplitude of true positive and false positive CCEPs (with respect to seizure propagation). Between these groups no significant differences were found. Furthermore they investigated the difference in propagation times between the true positive and false negative CCEPs. There was a tendency for the propagation times in the false negative group to be higher, but no consistent significant difference was found. From these results they concluded that there was no robust connection between CCEPs and ictal propagation. These findings are however in contrast to the results found in this study (i.e. the high specificity of SPES early responses in relation to seizure propagation). This discrepancy can be explained in multiple ways. First off they only investigated statistical differences in response characteristics, and less emphasis was placed on the actual localisation of those responses. Furthermore their approach to analysis was mainly sensitivity driven,

comparing true and false positive responses. True negatives were also a relevant outcome and those have not been analysed in the CCEP study. As can be seen from our results, sensitivity was lower than specificity. But our sensitivity in conjunction with the high specificity indicated that a relationship between responses and ictal propagation is present. When comparing our sensitivity to theirs (not explicitly mentioned but can be derived from the results), ours is generally higher. One of the explanations for this lies in the difference in stimulation paradigm mentioned when comparing our results to another CCEP study. The smaller pulse width causes CCEP amplitudes to decrease, making it more likely to miss them. Their efforts to increase signal to noise ratio by averaging over a higher number of pulses might compensate for this. On the other hand, if stimulus intensity is insufficient to excite all underlying tissue, some responses might not be evoked at all, possibly explaining CCEP missing true positive detections.

When considering response characteristics our average amplitudes can be found to be higher than in CCEP studies. This again is explained by the pulse width difference. With respect to response delays we note that our median delays are lower. This is easily explained by the fact that CCEP reports delay ranges from 9-199ms. By our standard any responses >100ms are no longer categorized as an early response, and are therefore ignored. This difference in analysed delay ranges accounts for our delay median being lower than in CCEP studies.

Clinical Data Limitations

Because the data were acquired within a clinical stimulation protocol there are some limitations to be considered. Due to the time consuming nature of the SPES protocol an important decision was made with respect to the polarity of the stimulation. The stimulator was plugged into a circuit board with plugs corresponding to the electrodes in the brain. Stimulation is carried out in a row by row fashion. To save time a single connector was re-plugged for each stimulation. This causes a single electrode to always have the same polarity (figure 3). It is known that tissue at the site of the cathode is excited more easily than at the site of the anode. The implications of this choice, made out of practical considerations, are unclear. If stimulation efficiency is increased one would expect more fibres to be excited with the same stimulus intensity, thus leading to more responses. If we hypothesize that these additional responses would be evenly divided between true and false positive responses we would find

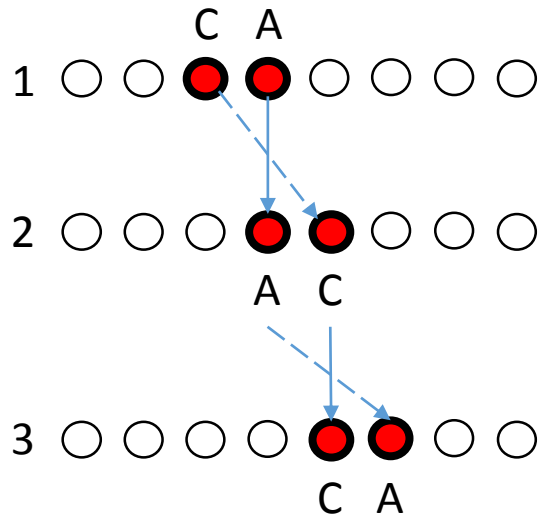

Figure 3 Explanation how a single electrode maintains the same polarity throughout the stimulation protocol. Situation one will be the first stimulation, C is the cathode, A the anode. In order to reduce the time taken to fully stimulate all grids, the anode remains connected between the two situations. The cathode is disconnected and reconnected to the electrode to the right of the anode. The third situation is obtained from the second in a similar way, the cathode remains connected and the anode is reconnected to a different electrode.

in increase in sensitivity, with a relatively lower decrease in specificity due to the ratio between electrodes involved in the seizure and those not involved. However it should be noted that this stimulation polarity issue occurs in 50% of the stimulated electrode pairs, thus the expected improvement in results would be relatively small.

Furthermore the electrode grids were placed by the neurosurgeon during the first surgical procedure. The aim of this intervention is to get the grid electrodes to cover as much of the suspect epileptic cortex as possible. However in that process less consideration is put in the anatomical positioning of the electrodes with respect to the gyri and sulci. Ideally the electrodes should be placed solely right on top of the gyri. For witnessing interictal and ictal events this is less crucial, but it can influence the effectiveness of the stimulation during a SPES protocol. When a given stimulation pair has one electrode situated above a sulcus it results in a loss of effective stimulation intensity and can lead to a smaller amount of cortical tissue to be excited. In recent literature efforts have been made to construct patient specific grid electrodes using the MRI data from any given patient. Subsequently, using 3D printed mould, silicone encased grid electrodes were created [27]. Ideally a similar technique should be used for SPES of the SOZ. This gives the neurologist more control over the areas that are to be stimulated. Correct electrode placement is paramount for optimal results and their reliability.

The above remark pertaining to the placement of the electrodes leads to another point of discussion. During the clinical SPES protocol electrodes are only stimulated in a row wise fashion. When the post-implantation MRI is inspected one could argue that in some cases a column wise stimulation would be more favourable due to the anatomical orientation of the underlying gyrus. One could argue that when anatomy is considered diagonal stimulation should also be considered, but that raises the problem of increased inter-electrode distance so that should be avoided. Again this limitation pertains to the efficiency of cortical stimulation. Increasing stimulation efficiency would increase the chance of evoking responses in the cortical tissue. This in turn would lead to an increase in this study's sensitivity and predictive values at the cost of a decrease in its specificity.

Algorithm limitations

The algorithm applied to remove the stimulation artefact also has its limitations. Even though it is able to show and detect responses on the slope of the stimulation artefact it still leaves a residual artefact in the filtered data. This residual artefact keeps us from detecting responses right after the stimulus is applied. To avoid false positive detection of this artefact we limited the detection window to >20ms after the stimulus. That leaves us with a 20 ms blind spot in which the artefact removal algorithm is not reliable. All responses detected outside of that window were within the same order of magnitude as reported in other SPES and CCEP studies [6, 10].

The algorithm devised to automatically process and analyze our data uses an amplitude threshold for its response detection. This threshold was initially set to 120µV for all patients and subsequently increased or decreased upon visual inspection of the data. It has been witnessed that response amplitudes have some variation from patient to patient. This could be explained by the localization of the stimulus site (e.g. frontal lobe vs. temporal lobe) or the general cortical excitability. Ideally the threshold should be defined equally for each patient. This would reduce a potential bias when determining an appropriate threshold. Whether or not a peak detection algorithm was necessarily the best choice is still under debate.

With the current implementation of our algorithm we only analyzed the first generation effective connectivity (i.e. areas showing a marked early response (B) to stimulation of the seizure onset zone (A)). In some of our results we observed that remote responses occur within a much larger region involved in the actual seizure (e.g. patient 6). In this case we hypothesize that this area could behave

as a secondary hub from which epileptic activity propagates along the neighbouring areas. In which case describing the effective network by means of A to B connectivity would not suffice. Our adjacency correction sought to correct for this phenomenon but more fundamental alterations in the analysis protocol might be more favourable.

SPES response latency

Questions should be asked with respect to the electrophysiological origin of SPES evoked responses. SPES is assumed to excite the cortico-cortical mu-fibres. Cortico-cortical information exchange should be among the most efficient neurological connections our body has to offer. However when SPES response latencies are observed our results show a median response time of 43ms. This is orders of magnitude higher than what would be expected. It is likely that responses are not just cortico-cortically propagated activations and that more parts of the brain (e.g. the thalamus) are involved in the generation of the actual response [7].

Conclusion

SPES early responses can be used to map the epileptic brain. When the seizure onset zone is stimulated the localization of responses is closely related to ictal propagation.

Future prospects

Even though there are some difficulties due to the retrospective nature of the data the results are promising. The fact that SPES responses can mimic electrical phenomena witnessed as much as 30 seconds into an ictal event is remarkable.

Previously a relationship was shown between the delayed SPES responses and the seizure onset zone. Since our study uses the knowledge of the seizure onset zone to predict the propagation behaviour of a seizure, combining delayed and early response evaluation would render us able to map the epileptic brain without the necessity of an actual seizure occurring.

Furthermore, evaluating early responses could be used in cases of multiple possible regions of seizure onset. When SPES is applied to these areas it is possible to compare the response localization to recorded ictal events. Subsequently the stimulated area whose responses resemble the actual ictal events closest would be more likely to be marked as the actual seizure onset zone. Though it will never replace the trained eye of an epileptologist SPES early responses show favourable characteristics, and due to their high specificity they could be used to help clinical decision making in difficult cases. More research into these topics is required.

References

1. Engel, J. and T.A. Pedly, *Epilepsy: A Comprehensive Textbook*. 2nd ed. Vol. 1. 2007: Lippincott Williams & Wilkins.
2. van 't Klooster, M.A., et al., *Time-frequency analysis of single pulse electrical stimulation to assist delineation of epileptogenic cortex.* Brain, 2011. **134**(Pt 10): p. 2855-66.
3. Battaglia, G., et al., *Periventricular nodular heterotopia: classification, epileptic history, and genesis of epileptic discharges.* Epilepsia, 2006. **47**(1): p. 86-97.
4. Jansen, F.E., et al., *Identification of the epileptogenic tuber in patients with tuberous sclerosis: a comparison of high-resolution EEG and MEG.* Epilepsia, 2006. **47**(1): p. 108-14.
5. Meroni, A., et al., *Nodular heterotopia: a neuropathological study of 24 patients undergoing surgery for drug-resistant epilepsy.* Epilepsia, 2009. **50**(1): p. 116-24.
6. Iwasaki, M., et al., *Accentuated cortico-cortical evoked potentials in neocortical epilepsy in areas of ictal onset.* Epileptic Disord, 2010. **12**(4): p. 292-302.
7. Matsumoto, R., et al., *Functional connectivity in human cortical motor system: a cortico-cortical evoked potential study.* Brain, 2007. **130**(Pt 1): p. 181-97.
8. Matsumoto, R., et al., *Functional connectivity in the human language system: a cortico-cortical evoked potential study.* Brain, 2004. **127**(Pt 10): p. 2316-30.
9. Valentin, A., et al., *Responses to single pulse electrical stimulation identify epileptogenesis in the human brain in vivo.* Brain, 2002. **125**(Pt 8): p. 1709-18.
10. Enatsu, R., et al., *Correlations between ictal propagation and response to electrical cortical stimulation: a cortico-cortical evoked potential study.* Epilepsy Res, 2012. **101**(1-2): p. 76-87.
11. Pijnenburg, Y.A., et al., *EEG synchronization likelihood in mild cognitive impairment and Alzheimer's disease during a working memory task.* Clin Neurophysiol, 2004. **115**(6): p. 1332-9.
12. Stam, C.J., G. Nolte, and A. Daffertshofer, *Phase lag index: assessment of functional connectivity from multi channel EEG and MEG with diminished bias from common sources.* Hum Brain Mapp, 2007. **28**(11): p. 1178-93.
13. Stam, C.J., et al., *Small-world networks and functional connectivity in Alzheimer's disease.* Cereb Cortex, 2007. **17**(1): p. 92-9.
14. Ponten, S.C., F. Bartolomei, and C.J. Stam, *Small-world networks and epilepsy: graph theoretical analysis of intracerebrally recorded mesial temporal lobe seizures.* Clin Neurophysiol, 2007. **118**(4): p. 918-27.
15. van Dellen, E., et al., *Long-term effects of temporal lobe epilepsy on local neural networks: a graph theoretical analysis of corticography recordings.* PLoS One, 2009. **4**(11): p. e8081.
16. Horstmann, M.T., et al., *State dependent properties of epileptic brain networks: comparative graph-theoretical analyses of simultaneously recorded EEG and MEG.* Clin Neurophysiol, 2010. **121**(2): p. 172-85.
17. Stam, C.J. and B.W. van Dijk, *Synchronization likelihood: an unbiased measure of generalized synchronization in multivariate data sets.* Physica D, 2002. **163**: p. 16.
18. Fingelkurts, A.A. and S. Kahkonen, *Functional connectivity in the brain--is it an elusive concept?* Neurosci Biobehav Rev, 2005. **28**(8): p. 827-36.
19. van Diessen, E., et al., *Does sleep deprivation alter functional EEG networks in children with focal epilepsy?* Front Syst Neurosci, 2014. **8**: p. 67.
20. Lesser, R.P., N.E. Crone, and W.R. Webber, *Subdural electrodes.* Clin Neurophysiol, 2010. **121**(9): p. 1376-92.
21. Jacobs, J., et al., *Interictal high-frequency oscillations (80-500 Hz) are an indicator of seizure onset areas independent of spikes in the human epileptic brain.* Epilepsia, 2008. **49**(11): p. 1893-907.
22. Jacobs, J., et al., *High-frequency electroencephalographic oscillations correlate with outcome of epilepsy surgery.* Ann Neurol, 2010. **67**(2): p. 209-20.

23. Spencer, S.S., *Cortical and intercortical seizure spread*, in *Anatomy of epileptogenesis*, B.S. Meldrum, J.A. Ferrendelli, and H.G. Wieser, Editors. 1988, Libbey.
24. Conner, C.R., et al., *Anatomic and electro-physiologic connectivity of the language system: a combined DTI-CCEP study.* Comput Biol Med, 2011. **41**(12): p. 1100-9.
25. Lacruz, M.E., et al., *Frontal and temporal functional connections of the living human brain.* Eur J Neurosci, 2007. **26**(5): p. 1357-70.
26. Alarcon, G., et al., *Intracerebral propagation of interictal activity in partial epilepsy: implications for source localisation.* J Neurol Neurosurg Psychiatry, 1994. **57**(4): p. 435-49.
27. Morris, S., et al., *Patient Specific Cortical Electrodes for Sulcal and Gyral Implantation.* IEEE Trans Biomed Eng, 2014.

Appendix A - Algorithm Implementation

Since single pulse responses can be contaminated by a large stimulus artefact an algorithm was devised to correct for this problem. The aims of this algorithm were formulated as follows:

- Automatic segmentation of the data into ten responses per stimulus pair
- Removal of the stimulation artefact
- Detection of early responses
- Visualisation of results

In the upcoming sections the implementations of these aims will be further elaborated.

Automatic segmentation

The basic concept of this part of the algorithm is to use peak detection to find the peaks of the stimulus artefact. The detection of the peaks occurs in two stages.

Region definition

In the first stage regions of interest were defined in which ten stimuli occur. To define these regions we first selected the channel of an electrode that was never used as a site of stimulation. This was done manually and upon visual inspection of the data. These electrodes were usually present in the data set. Artefact morphology was seen to be different when an electrode was actually stimulated, making them unfavourable for this primary step.

Subsequently a peak detection algorithm was used (N.C. Yoder, Matlab File-central). This algorithm finds local maxima above a user-defined threshold, but also considers the fact that not all local maxima are in fact relevant. For a peak to be returned as detected the data-point should also deviate from the surrounding data, making it more resistant to random fluctuations.

Now the approximate times of stimulation were known, the next step was to segment those into groups of stimuli related to a single given stimulation pair. The inter-stimulus interval was known through considering the fact that stimuli were applied with a frequency of 0.2 Hz. If the inter-stimulus interval was found to be 2 seconds or more overdue it was assumed that a new pair was stimulated from that point. Using this knowledge we could define the first and last stimuli of a stimulation pair. This gave us regions of interest (data sections) that each contain the ten stimuli applied to a single stimulation pair.

Individual stimulations

After regional segmentation individual pulses were detected on all electrodes. Using an iterative algorithm we evaluated all electrodes per defined region (i.e. stimulation pair). Since the stimulation artefact could sometimes switch polarity on different electrodes the algorithm applied slightly different sections of code depending on the mean value of the data. When the data mean was positive, the algorithm looked for positive values. In case of a negative mean, peaks would be searched in the negative data values.

If in any case duplicate detections were found (i.e. peaks <2 seconds apart, bearing in mind a 5 second inter-stimulus interval) we corrected by only retaining the first detected peak and ignoring subsequent duplicates.

A check was implemented to verify if indeed ten peaks were found on the given electrode. If this was not the case the algorithm made note of this by returning a message informing the user of the stimulation pair and the electrode on this detection failure had occurred.

Next, we selected a time window of [-0.1s 4s] around the detected peaks in the data from a single electrode given a single stimulus pair. This data was averaged into a ten pulse averaged stimulus response to be used in subsequent early response detection.

Artefact removal

Since the presence of stimulation artefacts posed a significant problem in detecting early responses these had to be removed. First and foremost it was important to understand that we do in fact have knowledge about the stimulation artefact. The morphology, though not the amplitude, was similar in almost all recorded channels. We intended make use of this knowledge in the process of devising an algorithm to remove artefacts.

Our artefact removal algorithm applied a first order wiener filter in order to reconstruct the artefact free signal. The concept of the filter is schematically illustrated in figure 1.

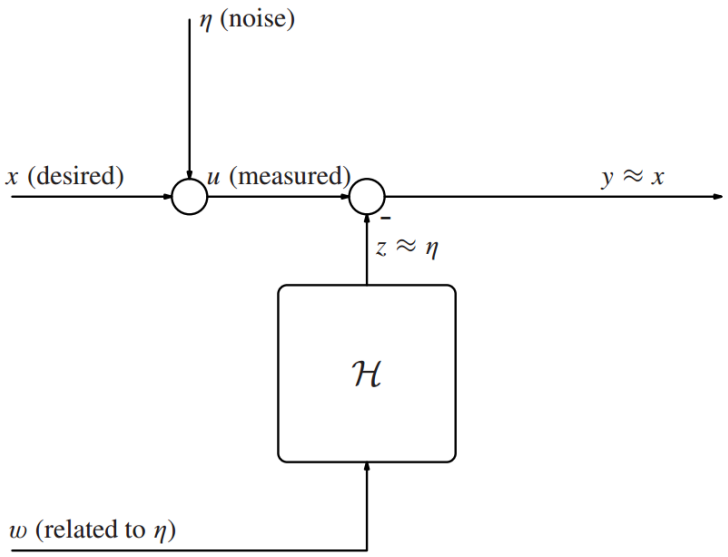

Figure 4 Basic schematic representation of the proposed filtering problem. x is our desired signal (artefact free response), η is the introduced stimulation artefact and ω will be constructed as a signal related to our η.

The problem posed here is to find a filter H that will create an estimate of our artefact. For this method to work x should not be correlated to either η or ω. In our case this was a safe assumption to make since we will construct ω ourselves based upon an estimate of η, which we will get back to later.

Solving the above problem was achieved by minimizing the power of η-z, pow(η-z). The smaller this residual power was the better our filter would be able to mimic the actual artefact. Of course we did not know η. However through the assumption that x was not correlated to either η or ω, the problem could be rewritten to be a matter of minimizing pow(u-z).

Subsequently the desired filter could be estimated by solving the Wiener-Hopf equations shown below. Here M is the order of the desired filter, r_ω is the autocorrelation function of ω, and $r_{u\omega}$ is the cross correlation function of u and ω.

$$\begin{bmatrix} r_\omega(0) & r_\omega(1) & \cdots & r_\omega(M) \\ r_\omega(1) & r_\omega(0) & \ddots & r_\omega(M-1) \\ \ddots & \ddots & \ddots & \vdots \\ r_\omega(M) & r_\omega(M-1) & \cdots & r_\omega(0) \end{bmatrix} \begin{bmatrix} h_0 \\ h_1 \\ \vdots \\ h_M \end{bmatrix} = \begin{bmatrix} r_{u\omega}(0) \\ r_{u\omega}(1) \\ \vdots \\ r_{u\omega}(M) \end{bmatrix}$$

Equation 1 The Wiener-Hopf equations, solving these results in the solution to our problem: minimizing pow(u-z).

Since u and ω are both known, the auto and cross correlation functions can be calculated. Now equation can be solved, yielding us the desired filter estimate h_*.

In order to solve the above equation a proper ω needs to be defined. It has to be similar to η, our stimulation artefact. First we state that given a single stimulation pair, there will always be many electrodes on which no response is recorded. Furthermore the morphology of the stimulus artefact is similar throughout all channels. A good first estimate of η would be to average the data of all recorded channels, excluding the ones that were used for the actual stimulation. This is a fair first estimate, but we need to keep in mind that when all channels are averaged, there will always be channels in which the data contains an early response. This contamination of ω with x introduces some inherent correlation between x and ω, which as was seen before is not allowed for the filter to work optimally. Since the influence of x on ω is relatively small, the filter will work, but improvements can be made. Ideally the channels showing a response should not be included in the construction of ω. Therefore we apply a first round of peak detection on the (sub-optimally) filtered data (we will get back to the specifics of this peak detection in the next section). Now that this peak detection has been performed, we have a first estimate of whether or not a channel contains a response. This knowledge is then used to refine the creation of ω. Again we create an average of all channels, but this time around we exclude the stimulated channels *and* the channels that showed a response in our first round of detection. This process is then repeated four times to further clean up our ω. Often one or two additional cycles were usually enough to find no new responding channels, but to be sure and improve applicability to future data sets the amount cycles was set to four. Through refining our ω we can now safely assume that ω is no longer correlated to x and our filter will work optimally.

Final early response detection

Now that we have a filtered, artefact free response signal we can move on to the final step, the detection of the actual early responses. It should be noted that sometimes a residual artefact remains, this impairs our ability to detect responses right after stimulation (figure 2).

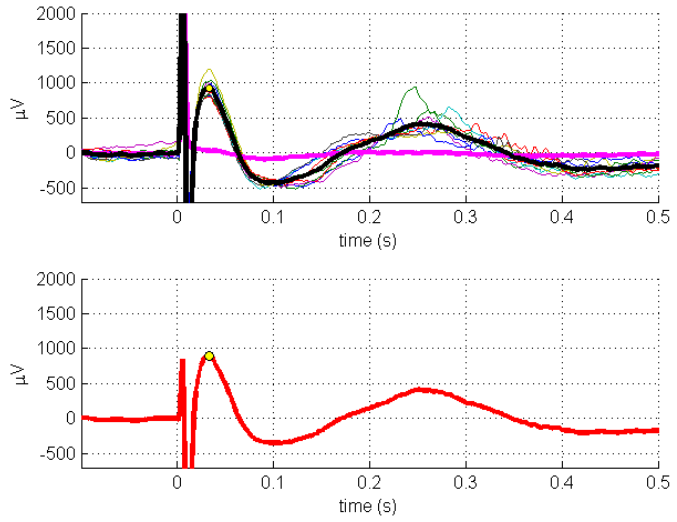

Figure 2 Results of the initial artefact removal. The original signals (multi-colored) and its average (black) are shown in the top graph. The artefact morphology estimate template is shown in magenta. In the bottom figure the red graph shows the results of the artefact removal algorithm. Note that the detected early response is shown as a yellow circle.

A detection delay was implemented. In practice this means that peaks will only be detected 20 ms after the stimulus is applied. For the detection of the early responses the aforementioned peakfinder algorithm was utilized again (Appendix A, p.26, Region Definition). For its detection threshold we refer back to the methods in the main section. To make sure the detected peaks are not random data spikes the signal on which peaks are detected was first run through a seven sample running average filter (figure 3). The detected peaks were then corrected for possible induced time offset and projected back to the original Wiener filtered signal. This way the detection is less susceptible to random spikes, but the response latency and amplitude remain reliable since the peaks are projected back to an unaveraged signal.

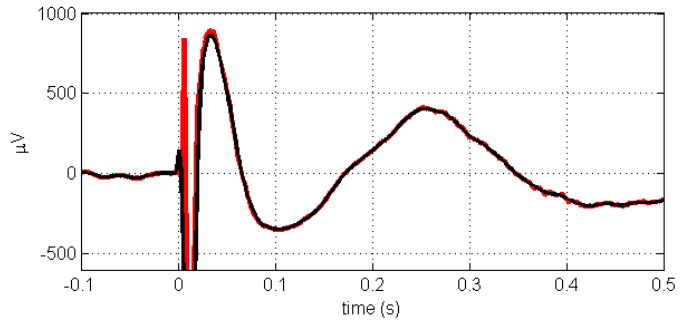

Figure 3 The effects of the seven sample running average filter on the post-artefact removal signal. The signal with its reduced artefact is shown in red and the seven sample averaged signal is shown in black. Note that the residual artefact spike is removed by this averaging filter, allowing for more accurate response detection.

Finally, for aesthetic purposes we opt to remove the residual artefact by applying a cubic interpolant between 0 and 20 ms, since this is a section of data that is not used for peak detection or any other operations (figure 4).

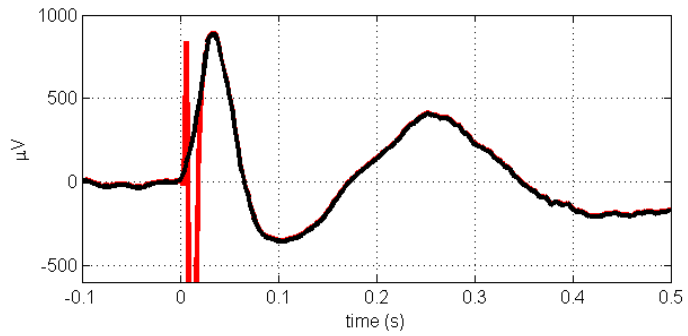

Figure 4 The result of the cubic interpolant to remove the residual artefact for aesthetic purposes. The signal containing the residual artefact is shown in red and the result of the cubic interpolant is shown in black.

Visualization of results

For an easy interpretation of results it was thought necessary to return the results of early response detection in a way that more closely represents the anatomical relationship of the recorded electrodes. We will refer to this as the creation of topographical maps. In clinical practice excel sheets are often created to give schematic overviews of the spatial relationship between the different grid and strip electrodes. The elements in these excel sheets contain the numbers of the channels the electrodes were recorded on. This was used as a starting point for visualization, but the aim is to give the final visualization a more organic feel to it. We will now demonstrate the steps taken to come to the final result based on an example.

First we start off with the excel sheet containing the channel numbers. We manually fill up the empty elements with zeroes so that the entire sheet is filled up with real numbers (otherwise importing the sheet through the Matlab command xlsread will not function) this is shown in figure 5.

0	0	0	0	0	0	0	0	0	0	0	0	0	0	0	0
0	0	65	66	67	68	69	70	71	72	0	0	0	0	0	0
0	0	0	0	0	0	0	0	0	0	0	0	0	0	0	0
0	0	64	63	62	61	60	59	58	57	0	0	0	0	0	0
0	0	56	55	54	53	52	51	50	49	0	0	0	0	0	0
0	0	48	47	46	45	44	43	42	41	0	0	0	0	0	0
0	0	40	39	38	37	36	35	34	33	0	0	0	0	0	0
0	0	32	31	30	29	28	27	26	25	0	0	0	0	0	0
0	0	24	23	22	21	20	19	18	17	0	0	0	0	0	0
0	0	16	15	14	13	12	11	10	9	0	80	79	78	77	0
0	0	8	7	6	5	4	3	2	1	0	76	75	74	73	0
0	81	82	83	84	0	96	0	0	0	0	0	0	0	0	0
0	85	86	87	88	0	95	0	0	0	0	0	0	0	0	0
0	0	0	0	0	0	94	0	0	0	0	0	0	0	0	0
0	0	0	0	0	0	93	0	0	0	0	0	0	0	0	0
0	0	0	0	0	0	0	0	0	0	0	0	0	0	0	0

Figure 5 The contents of an excel sheet with schematic representation of the spatial relationship of the electrodes.

Subsequently this sheet is imported into Matlab, this is the variable topo.template. From this variable we store the locations of all the electrodes in this matrix into a variable called topo.loc. Next we create a binary matrix through topo.template>0. This is a miniature black and white image shown below.

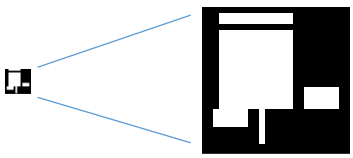

Figure 6 Black and white intermediate image. The right one is slightly zoomed in since the original size makes the individual black and white pixels barely visible.

It goes without saying that this image is not usable to visualize data due to its size. We need to resize this. Also we would like to have just the outline of the grids. This will be achieved through the following line of code:

```
BW = edge(imresize(topo.template>0+0,fact),'canny');imshow(1-BW);
```

In this line BW stands for a black-white representation of the grid. Edge refers to the command that will find the edges of the resized matrix. For image interpolation we use the canny interpolation option. The variable fact is the resize factor from the intermediate image shown in figure 6 to the final map outline. Since BW is now a black image with a white line marking the outline we need to invert it through the operation 1-BW. The image resulting from this code looks as follows:

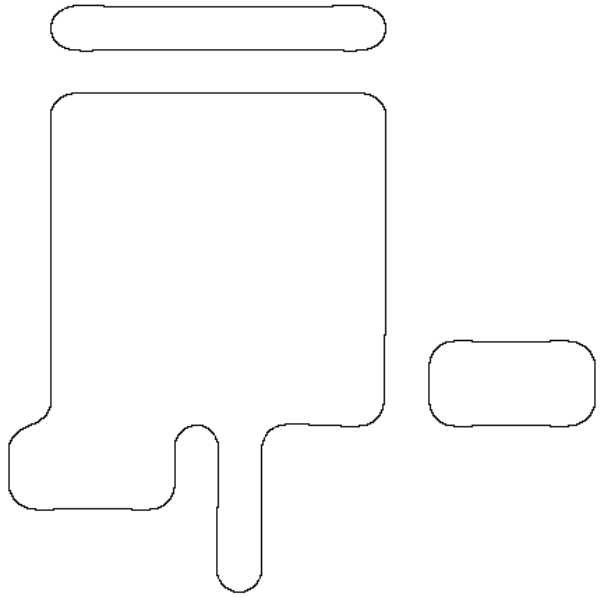

Figure 7 The resulting outline of our grid electrodes

Now all that remains is to plot the electrodes at their respective positions. Since a resize was implemented the positions of the electrodes have changed with respect to figure 6. The corrections were made using the following equations to transform the old row (r) and column (c) indices into their new, post-resize versions.

$$r_{new} = r_{old} * fact - \frac{fact}{2}$$

$$c_{new} = c_{old} * fact - \frac{fact}{2}$$

Possessing the corrected row and column indices it is now possible to plot the electrodes at their correct positions. Doing so finalizes the topographic visualization of the grid and strip electrodes.

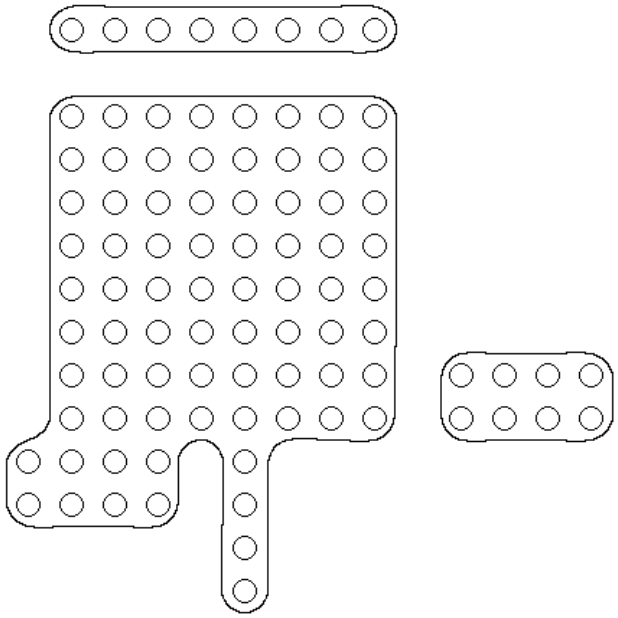

Figure 8 The final result of our conversion of an excel sheet into a useful topographic map of the electrode positions

Graphical User Interface

The amount of data that needed to be analysed and inspected was staggering. Therefore we aimed to create a GUI as a tool to make the inspection faster and more intuitive. For instance, given a single stimulation pair, there were a lot of channels of which one would like to see the recorded data. Also the number of stimulation pairs was rather large. To cope with that the GUI needed to be able to:

- Visualize data of a single stimulation pair in a way that the behaviour of single channels could be easily recognizable.
- Switch between the data of stimulation pairs quickly and easily
- Offer the option to visualize the data from channels of interest.

In short the aim was to create a natural feeling data browser. The best way to explain how this was done is by showing the GUI and explaining its different elements.

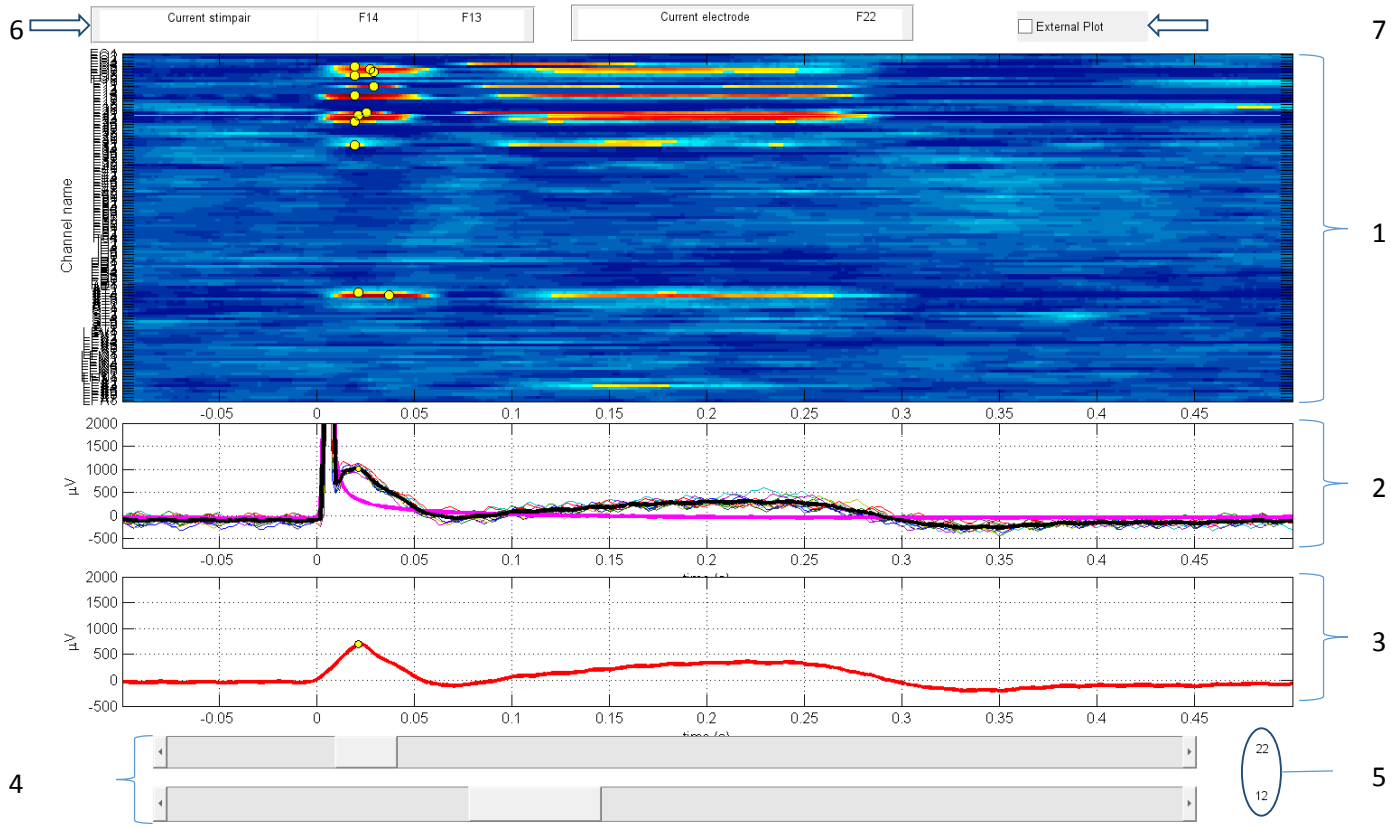

Figure 9 The GUI window as it was created. Numbered accolades and arrows show its features and elements of notice.

Based on the numbering in figure 6 we will now go over the GUI interface, its controls and its features.

1) The birds-eye view of the data recorded from the current stimulation pair. The y-axis shows the individual channels (labelled by importing the channel names from the TRC file). The x-axis is time in seconds. The axis x-label is present but due to rescaling to fit the page of this report it is no longer visible. Colours indicate signal intensity of a given channel in any point in time. Red indicates high amplitude and blue indicates low amplitude. Note that the data plotted here is already corrected for the stimulus artefact. Yellow dots show the detected early responses in this particular stimulation pair.

   Element 1 shows an overview in which it is possible to get a first impression of detected early responses. Red areas (high amplitude) indicate that a response is likely, subsequently one can check whether or not these red areas have been marked with a yellow dot (detected early), and further investigate those channels of interest.

   Finally there is a horizontal white line that indicates the channel of which the data is currently visualized in elements 2 and 3. Though not easily visible in the above figure, it is in fact easily recognizable in Matlab. It gives the user an indication on how far to move the sliders (element 4) to select the channel from which they want to inspect the data.

2) The second set of axes gives an indication of the original data. Multiple things are plotted here, first the 10 individual pulse responses are shown (the more noisy signals that can be seen). Second it shows the 10 pulse averaged response in black. It also shows the estimated (removed) stimulation artefact in pink. Finally the detected response (if available) is also

plotted, again with a yellow dot. Also mind that the scaling of the x-axis is identical to that of element 1, further facilitating data inspection.

3) This element shows the estimated response (i.e. the signal after artefact removal) in red. Again it shows the detected early response with the known yellow dot. Like in element 2 we kept the scaling of the x-axis identical to make it easier to compare the original and filtered signals.

4) The sliders in element 4 are the main controls of this GUI. The top one selects a channel within the selected stimulation pair. The slider properties (the min and max value) are automatically set based on the properties of the data set.

   The bottom controls the selection of the stimulation pair of which the data is to be visualized. Again the properties are automatically acquired from the data set.

5) This is an indicator showing the current value of the sliders. These values are channel number and stimulation pair, corresponding to their sliders.

6) In addition to the numerical indicators next to the sliders (element 5) this element shows the channel labels of the currently selected channel and stimulation pair.

7) If the user wants to save the current contents of elements 2 and 3 to a separate figure, this button allows them to do so. The button creates a new figure in which copies of the contents and properties of the axes-objects of element 2 and 3 and all their properties are copied. Also, in this new figure, the axes of the two plots are linked, meaning that zooming in either, applies the same transformation in the other. Scrolling through the plot works in a similar manner, moving one subplot automatically translates the other too.

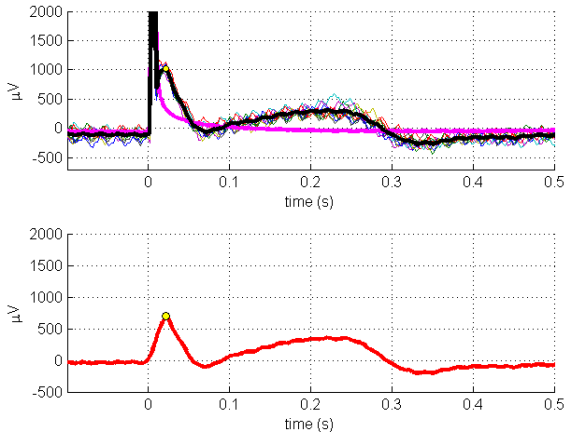

Figure 5 Example of the external figure created by the checkbox (element 7 of the GUI).